On-chip TIRF nanoscopy by applying Haar wavelet kernel analysis on intensity fluctuations induced by chip illumination: supplement

NIKHIL JAYAKUMAR,[1,3] ØYSTEIN I. HELLE,[1] KRISHNA AGARWAL,[1] (iD) AND BALPREET SINGH AHLUWALIA[1,2,4] (iD)

[1]*Department of Physics and Technology, UiT The Arctic University of Norway, Tromsø 9037, Norway*
[2]*Department of Physics, Indian Institute of Technology Delhi, Hauz Khas, New Delhi 110016, India*
[3]*nik.jay.hil@gmail.com*
[4]*balpreet.singh.ahluwalia@uit.no*

On-chip TIRF nanoscopy by applying Haar wavelet kernel analysis on intensity fluctuations induced by chip illumination : supplemental document

S1. *HAWK transform*

Consider the situation of a single pixel which has an intensity trace of 4 frames. This data

stack of 4 frames in general may be represented as $\begin{pmatrix} a \\ b \\ c \\ d \end{pmatrix}$. The corresponding transformed

intensity $\begin{pmatrix} p \\ q \\ r \\ s \end{pmatrix}$ trace can be obtained after multiplication with a 4×4 Haar matrix as shown

below.

$$
\begin{bmatrix} \frac{1}{2} & \frac{1}{2} & \frac{1}{2} & \frac{1}{2} \\ \frac{1}{2} & \frac{1}{2} & -\frac{1}{2} & -\frac{1}{2} \\ \frac{1}{\sqrt{2}} & -\frac{1}{\sqrt{2}} & 0 & 0 \\ 0 & 0 & \frac{1}{\sqrt{2}} & -\frac{1}{\sqrt{2}} \end{bmatrix} \begin{pmatrix} a \\ b \\ c \\ d \end{pmatrix} = \begin{pmatrix} \frac{a+b+c+d}{2} \\ \frac{a+b-c-d}{2} \\ \frac{a-b}{\sqrt{2}} \\ \frac{c-d}{\sqrt{2}} \end{pmatrix} = \begin{pmatrix} p \\ q \\ r \\ s \end{pmatrix}
$$

The next step is to apply the desired filter level *m*. The possible values of *m* are integers in the range 1 to $\log_2 N$, where N is the total number of frames in the original data stack. The filtered pixel intensity trace can be calculated by applying the condition $H^{-1} = H^T$ to

get the resultant vector $\begin{pmatrix} F1 \\ F2 \\ F3 \\ F4 \end{pmatrix}$.

$$
\begin{bmatrix} \frac{1}{2} & \frac{1}{2} & \frac{1}{\sqrt{2}} & 0 \\ \frac{1}{2} & \frac{1}{2} & -\frac{1}{\sqrt{2}} & 0 \\ \frac{1}{2} & -\frac{1}{2} & 0 & \frac{1}{\sqrt{2}} \\ \frac{1}{2} & -\frac{1}{2} & 0 & -\frac{1}{\sqrt{2}} \end{bmatrix} \begin{pmatrix} p \\ q \\ r \\ s \end{pmatrix} = \begin{pmatrix} \frac{p}{2} + \frac{q}{2} + r/\sqrt{2} \\ \frac{p}{2} + \frac{q}{2} - r/\sqrt{2} \\ \frac{p}{2} - \frac{q}{2} + s/\sqrt{2} \\ \frac{p}{2} - \frac{q}{2} - s/\sqrt{2} \end{pmatrix} = \begin{pmatrix} F1 \\ F2 \\ F3 \\ F4 \end{pmatrix} = \begin{pmatrix} a \\ b \\ c \\ d \end{pmatrix}
$$

For m = 1 the resultant vector is:

$$\begin{pmatrix} F1 \\ F2 \\ F3 \\ F4 \end{pmatrix} = \begin{pmatrix} \dfrac{(a-b)}{2} \\ \dfrac{-(a-b)}{2} \\ \dfrac{(c-d)}{2} \\ \dfrac{-(c-d)}{2} \end{pmatrix}$$

For m = 2 the resultant vector is:

$$\begin{pmatrix} F1 \\ F2 \\ F3 \\ F4 \end{pmatrix} = \begin{pmatrix} \dfrac{(a+b)}{4} - \dfrac{(c+d)}{4} \\ \dfrac{(a+b)}{4} - \dfrac{(c+d)}{4} \\ \dfrac{-(a+b)}{4} + \dfrac{(c+d)}{4} \\ \dfrac{-(a+b)}{4} + \dfrac{(c+d)}{4} \end{pmatrix}$$

The resultant vectors are then appended together to get the HAWK processed data stack. HAWK plugin in Fiji takes the desired filter level m as input from the user. After processing using HAWK, the negative values in the processed data stack are redressed positive or the positive and negative values are separated into two stacks and negative values are redressed positive. For the experiments presented in this manuscript, the latter condition is chosen with filter level $m = 3$.

S2. *A simple numerical example to illustrate the effect of the transform levels of HAWK*

To understand the influence of HAWK on the original image stack, consider a temporally varying signal such as $\begin{pmatrix} a \\ b \\ c \\ d \end{pmatrix} = \begin{pmatrix} 100 \\ 10 \\ 15 \\ 12 \end{pmatrix}$. This intensity trace is an example of a pixel lying on the border of a bright-dark band of the MMI pattern. The intensity trace of a pixel over time varies in proportion with the illumination intensity as the MMI pattern shifts transversally. The transformed traces for this particular pixel are $\begin{pmatrix} 45 \\ -45 \\ 1.5 \\ -1.5 \end{pmatrix}$ for $m = 1$ and $\begin{pmatrix} 20.75 \\ 20.75 \\ -20.75 \\ -20.75 \end{pmatrix}$ for $m = 2$. It can be seen that if the original data stack is used for SOFI reconstruction, this particular pixel will be rendered dim in the SOFI reconstructed image compared to pixels lying on a bright fringe. But after processing with HAWK the transformed intensity trace can lead to a higher pixel value in the SOFI reconstructions thereby aiding in alleviating the reconstruction artifacts due to the MMI pattern.

Similarly, an emitter lying on a bright band of the MMI pattern over the entire sequence of four frames can be represented as $\begin{pmatrix} 100 \\ 86 \\ 95 \\ 90 \end{pmatrix}$. This corresponds to an emitter exhibiting fluctuations with low temporal frequency. The transformed traces for such a pixel are $\begin{pmatrix} 7 \\ -7 \\ 2.5 \\ -2.5 \end{pmatrix}$ for $m = 1$ and $\begin{pmatrix} 0.25 \\ 0.25 \\ -0.25 \\ -0.25 \end{pmatrix}$ for $m = 2$. The non-linear response of SOFI images to brightness is therefore reduced after HAWK which helps prevent masking of the weaker emitters.

Lastly, let us consider an emitter exhibiting high temporal fluctuations. It can be represented as $\begin{pmatrix} 100 \\ 16 \\ 95 \\ 10 \end{pmatrix}$. The corresponding transform traces are $\begin{pmatrix} 42 \\ -42 \\ 42.5 \\ -42.5 \end{pmatrix}$ for $m = 1$ and $\begin{pmatrix} 2.75 \\ 2.75 \\ -2.75 \\ -2.75 \end{pmatrix}$ for $m = 2$. It can be seen that a highly fluctuating signal is represented predominantly by $m = 1$ filter while low temporal frequency information of emitters is retained by the higher order filter levels. Therefore, by appropriately choosing the filter level the artifacts generated by SOFI due to MMI patterns can be alleviated via HAWK processing. Ideally the correct filter level has to ensure that all the emitters get adequately represented in the reconstructed image.

S3. *HAWK helps depopulate regions with higher fluorophore density and increases the fluctuations*

The next challenge for SOFI is in reconstructing those regions of the sample, which have high fluorophore density. A high fluorophore density yields lower fluctuations, which in turn leads to a lower pixel value in the SOFI reconstructions. This is experimentally demonstrated by Fig. S1. For this particular experiment, Alexa Fluor 647 is coated on a Tantalum pentoxide waveguide surface. Images are acquired every 30 ms in epi-fluorescence mode. A region with a high density of fluorophores as shown in Fig. S1 is chosen and the ratio of standard deviation to average over 300 frames is calculated. The same data stack of 300 frames is then processed using HAWK and the ratio of standard deviation to average is again calculated. The filter level $m = 3$ is chosen so as to match with the experimental particulars described in the main article. It can be seen that the ratio of standard deviation to average increased two orders of magnitude for this experiment after the application of HAWK.
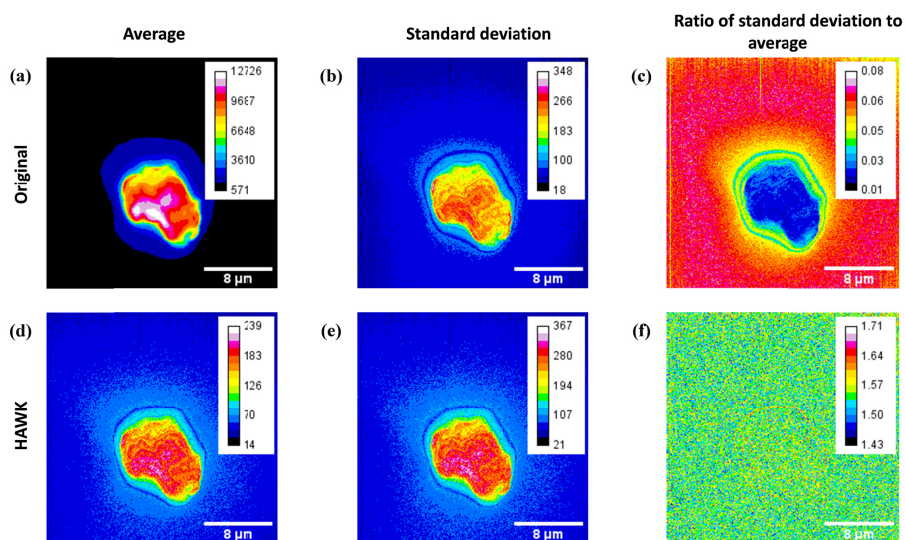
Fig. S1: Influence of HAWK on densely packed fluorophores. (a) Average of 300 frames. (b) Standard deviation over 300 frames. (c) Ratio of standard deviation to average over 300 frames. (d) Average of 1778 frames after HAWK processing. (e) Standard deviation of 1778 frames generated using HAWK. (e) Ratio of standard deviation to average of 1778 frames generated using HAWK. Scale bar 8 μm.

While imaging in waveguide TIRF mode, the fluctuations necessary for performing a SOFI reconstruction may arise from the intrinsic photokinetics of the fluorescent molecules as well as due to the oscillating nature of the illuminating scheme employed. To see which effect dominates, the following two experiments were performed. A uniform layer of Alexa Fluor 647 is coated on a Tantalum pentoxide waveguide and imaged as described in Section 2.1 of the main text.

In the first experiment, the coupling objective was held stationary and a stack of 300 frames were acquired. It means that the fluctuations recorded in the image stack arise only due to the intrinsic photokinetics of the fluorescent molecules. The results are presented in Fig. S2. For the second experiment, the coupling objective was manually oscillated and a sequence of 300 images were acquired during this process. Now the intensity trace of the pixels in the image frames so recorded will have fluctuations arising due to the intrinsic photokinetics of the fluorescent molecules as well as due to the oscillating nature of the illumination. The experimental results are presented in Fig. S3.
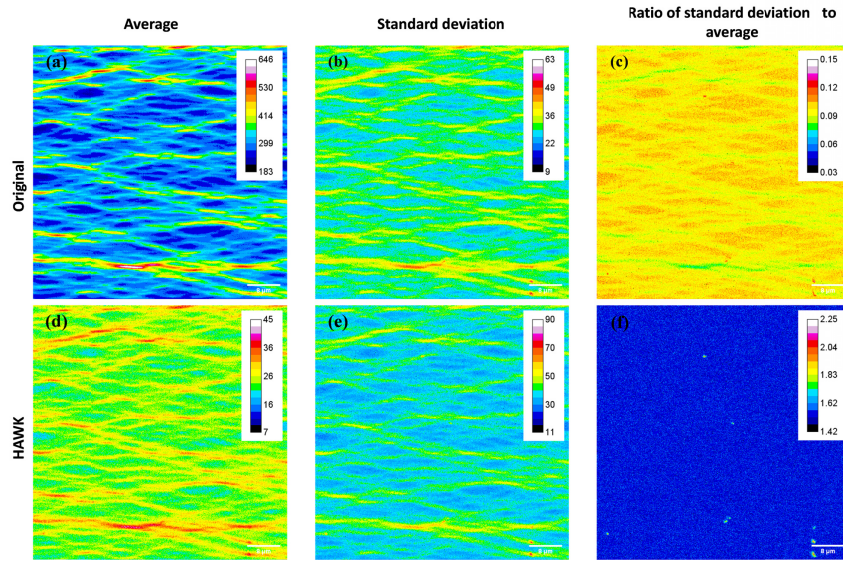
Fig. S2: Fluctuations due to intrinsic photokinetics in waveguide TIRF mode. (a) Average TIRF image of 300 frames. (b) Standard deviation over 300 frames. (c) Ratio of standard deviation to average of the original data stack of 300 frames. (d) Average TIRF image of HAWK processed data stack of 1778 frames. (e) Standard deviation over 1778 frames. (f) Ratio of standard deviation to average of the HAWK processed data stack of 1778 frames. Scale bar 8 μm.

It is seen from Fig. S2(c) and S2(f) that the ratio of standard deviation to average increased after the application of HAWK on the original data stack of 300 frames. Also, it can be seen from Fig. S2(c) and Fig. S3(c) that the fluctuations have been enhanced because of the oscillating illumination scheme employed.
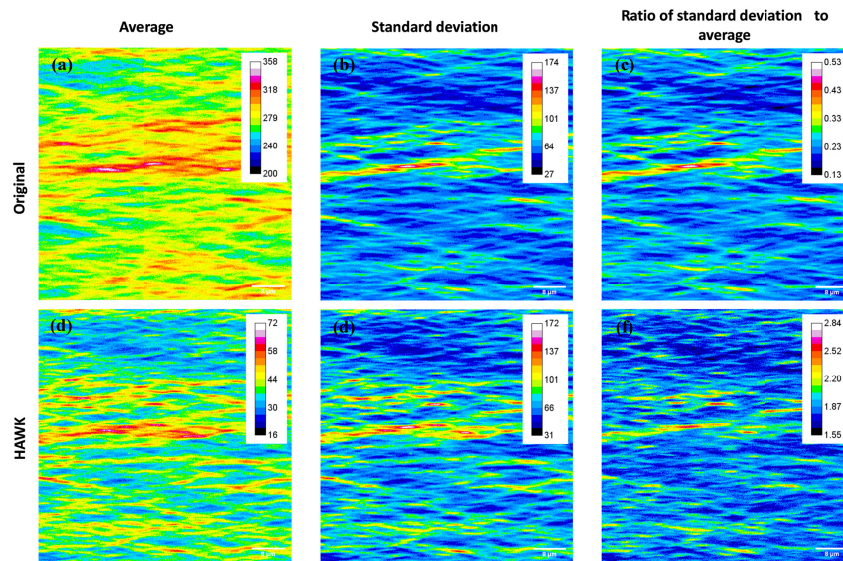

Fig. S3: Fluctuations due to intrinsic photokinetics and oscillating nature of illumination. (a) Average TIRF image of 300 frames. (b) Standard deviation over 300 frames. (c) Ratio of standard deviation to average of the original data stack of 300 frames. (d) Average TIRF image of HAWK processed data stack of 1778 frames. (e)

Standard deviation over 1778 frames. (f) Ratio of standard deviation to average of the HAWK processed data stack of 1778 frames. Scale bar 8 μm.

The inferences from these experiments is that in waveguide TIRF imaging mode, fluctuations arising due to photokinetics and waveguide illumination are present. It is also seen that HAWK helps in increasing the ratio of standard deviation to average in waveguide TIRF imaging mode and in regions with high density of fluorophores as shown in Fig. S1. It means that the necessity of averaging out the modes to generate a uniformly illuminated image can be exploited by HAWK to enhance intensity fluctuations even in regions having high density of fluorophores, thereby alleviating the reconstruction artifacts of SOFI due to MMI patterns.

S4. *Effect of different transformation levels of HAWK on the reconstruction quality*
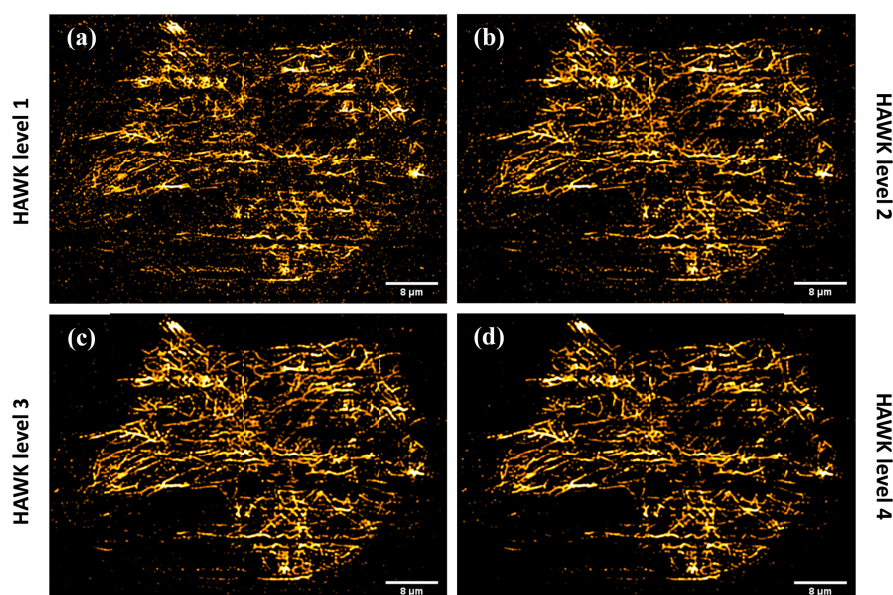

Fig. S4: Influence of HAWK filter levels on 4th order SOFI reconstruction. 4th order SOFI reconstructions on (a) HAWK data stack with m = 1, (b) HAWK data stack with m = 2, (c) HAWK data stack with m = 3 and (d) HAWK data stack with m = 4. Scale bar 8 μm.

Fig. S4 portrays the effect of HAWK filter levels on SOFI reconstructions. It can be seen that the HAWK data stack with m = 3 gave the best 4th order SOFI reconstruction. At low filter levels such as m = 1, the high temporal frequency content is more dominant as explained in Section 1.2. At higher filter levels, the low frequency information will also get adequately represented in the image stack. At even higher filter levels like m = 4 and above we expect the emitters exhibiting low temporal frequency with high intensity to be predominantly represented after the SOFI reconstructions due to the non-linear brightness scaling of SOFI. In this manuscript, m = 3 gave the best reconstruction.

S5. *Effect of the method of separation of negative values available in HAWK Fiji plugin on SOFI reconstruction*
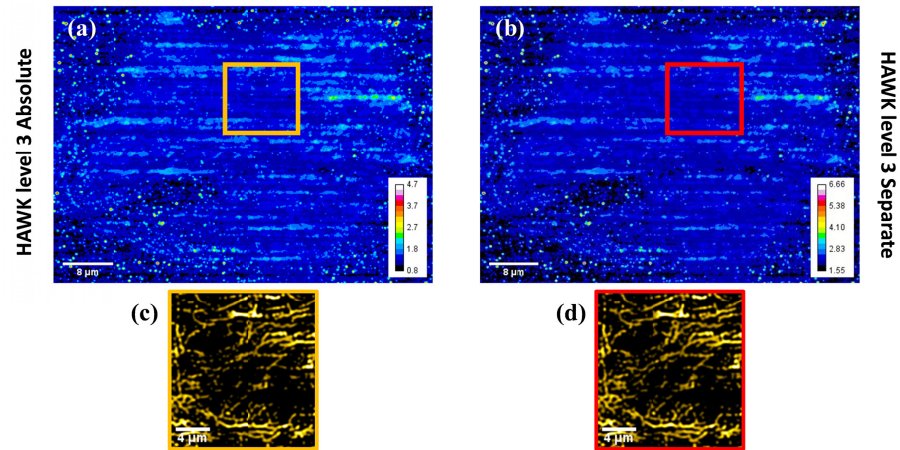

Fig. S5: Ratio of standard deviation to average on (a) HAWK data stack with absolute option used, (b) HAWK data stack with ''separate'' option used. 4th order SOFI reconstruction carried out on (c) HAWK data stack enclosed by the yellow box, (d) HAWK data stack enclosed by the red box. Scale bars: (a-b) 8 μm and (c-d) 4 μm.
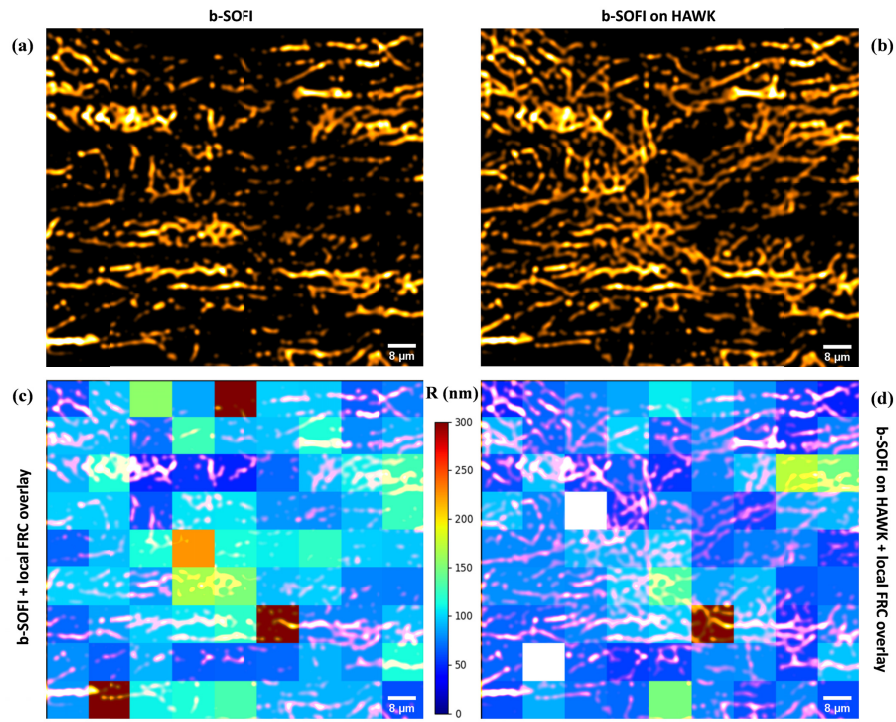
Fig. S6: Local FRC resolution for the data of Fig. 7. (a) b-SOFI reconstruction of the original data stack. (b) b-SOFI reconstruction on HAWK data stack. (c) Local FRC resolution R(nm) computed for 100×100 pixels on b-SOFI reconstruction of original data stack with b-SOFI reconstruction overlaid. (d) Local FRC resolution computed for 100×100 pixels on b-SOFI reconstruction of HAWK data stack with b-SOFI on HAWK reconstruction overlaid. The local FRC images are rescaled using bilinear interpolation before overlaying them with b-SOFI reconstructions. The pure white pixels indicate regions where local FRC failed to give a value. Scale bar: 8 μm.